BRAIN
ORIGINAL ARTICLE

Functional maps of direct electrical stimulation-induced speech arrest and anomia: a multicentre retrospective study

Junfeng Lu,[1,2,3,†] Zehao Zhao,[1,3,†] Jie Zhang,[1,3] Bin Wu,[3] Yanming Zhu,[3] Edward F. Chang,[4] Jinsong Wu,[1,2,3,5] Hugues Duffau[6] and Mitchel S. Berger[4]

†These authors contributed equally to this work.

Direct electrical stimulation, the transient 'lesional' method probing brain function, has been utilized in identifying the language cortex and preserving language function during epilepsy and neuro-oncological surgeries for about a century. However, comparison of functional maps of the language cortex across languages/continents based on cortical stimulation remains unclear.

We conducted a retrospective multicentre study including four cohorts of direct electrical stimulation mapping from four centres across three continents, where three indigenous languages (English, French and Mandarin) are spoken. All subjects performed the two most common language tasks: number counting and picture naming during stimulation. All language sites were recorded and normalized to the same brain template. Next, Spearman's correlation analysis was performed to explore the consistency of the distributions of the language cortex across centres, a kernel density estimation to localize the peak coordinates, and a hierarchical cluster analysis was performed to detect the crucial epicenters. A total of 598 subjects with 917 speech arrest sites (complete interruption of ongoing counting) and 423 anomia sites (inability to name or misnaming) were included.

Different centres presented highly consistent distribution patterns for speech arrest (Spearman's coefficient r ranged from 0.60 to 0.85, all pair-wise correlations $P < 0.05$), and similar patterns for anomia (Spearman's coefficient r ranged from 0.37 to 0.80). The combinational speech arrest map was divided into four clusters: cluster 1 mainly located in the ventral precentral gyrus and pars opercularis, which contained the peak of speech arrest in the ventral precentral gyrus; cluster 2 in the ventral and dorsal precentral gyrus; cluster 3 in the supplementary motor area; cluster 4 in the posterior superior temporal gyrus and supramarginal gyrus. The anomia map revealed two clusters: one was in the posterior part of the superior and middle temporal gyri, which peaked at the posterior superior temporal gyrus; and the other within the inferior frontal gyrus, peaked at the pars triangularis.

This study constitutes the largest series to date of language maps generated from direct electrical stimulation mapping. The consistency of data provides evidence for common language networks across languages, in the context of both speech and naming circuit. Our results not only clinically offer an atlas for language mapping and protection, but also scientifically provide better insight into the functional organization of language networks.

1 Glioma Surgery Division, Neurologic Surgery Department, Huashan Hospital, Shanghai Medical College, Fudan University, Shanghai 200040, China
2 Shanghai Key Laboratory of Brain Function Restoration and Neural Regeneration, Shanghai 200040, China
3 Brain Function Laboratory, Neurosurgical Institute of Fudan University, Shanghai 200040, China
4 Department of Neurological Surgery, University of California, San Francisco, CA 94143, USA
5 Institute of Brain-Intelligence Technology, Zhangjiang Lab, Shanghai 201210, China

6 Department of Neurosurgery, Gui de Chauliac Hospital, Montpellier University Medical Center, Montpellier 34295 CEDEX 5, France

Correspondence to: Prof. Jinsong Wu, MD, PhD
Glioma Surgery Division, Neurologic Surgery Department, Huashan Hospital
Shanghai Medical College, Fudan University
No. 12 Middle Wulumuqi Rd., Shanghai, China
E-mail: wujinsong@huashan.org.cn; wjsongc@126.com

Introduction

Since the establishment of the 'Montreal procedure', direct cortical electrical stimulation (DES) under awake craniotomy has been used to map and preserve the language cortex during epilepsy and neuro-oncological surgeries for about 100 years.[1] It was optimized by Penfield,[1] then subsequently introduced into the modern era by Ojemann,[2] and popularized in recent years.[3–7] The reliability and effectiveness of this technique in reducing persistent aphasia, has been exhibited during brain surgeries.[4,8–10] Although the mechanism of stimulation effects is poorly understood,[11] intraoperative language mapping has been widely considered as the 'gold standard' in localizing language areas and achieving maximal safe resection, based on its clinical relevance. It probes the causal relationship between brain regions and language function by directly, transiently and repeatedly interrupting language processing.[10] Therefore, the brain regions identified by DES represent the critical and essential areas, about a given function.

Several medical centres have separately established their native language maps using different templates.[1,3,6,7] However, whether the language maps across different languages or geographical continents shared the same distribution pattern remains unclear. Furthermore, the precise distribution may be affected by the potential differences in stimulus parameters, mass effects (tumour or epileptic lesion), brain plasticity (low-grade, high-grade glioma, and epilepsy),[12] normalization methods (from intraoperative individual cortex to standard space). Hence, there is an urgent need to establish a language map by integrating a large sample of DES data around the world.

In the present study, we included four DES cohorts from the past century from four centres across three continents, where three indigenous languages (English, French, and/or Mandarin) are spoken. All centres performed the two most commonly used paradigms (counting and picture naming). The corresponding stimulation-induced disruptions were identified as speech arrest and anomia. Speech arrest was defined as the complete interruption of the ongoing number counting or continuous speaking, without apparent oral, facial, jaw, or tongue movements. Anomia was defined as the DES-induced inability to name an object or misnaming using the wrong word, while still being able to speak the initial words, [i.e. 'This (picture) is a(n) …']. Finally, 598 subjects were included in further analyses, and the spatial distribution maps of speech arrest and anomia were generated respectively using the same template. The goal of the present study was to draw the functional map of the language cortex. Relevant questions included: (i) how the distributions of language cortex correlate across centres; (ii) which and how many regions are essential to stimulation-induced speech arrest; and (iii) which and how many regions are critical to stimulation-induced anomia; and (iv) what is the spatial relationship between speech arrest and anomia?

Materials and methods

Literature screening strategy

We aimed to identify all studies that reported the two most common intraoperative DES-induced disturbances (speech arrest and anomia), with a sample size of more than 50 cases and had available coordinates of positive language sites on the left hemisphere, irrespective of the language and study design. We searched PubMed, Web of Science and EMBASE databases for studies between 1 January 1946 and 15 February 2020, using a query combining the keywords: 'language OR arrest OR anarthria OR anomia OR dysnomia OR semantic OR speech' OR 'naming error' (response-related) with 'intraoperative stimulation mapping' OR 'direct cortical stimulation' OR 'direct electrical stimulation' NOT 'transcranial' (treatment-related). Relevant reviews, editorials, books and reference lists were also assessed for potential interest, where one study was identified. The identified studies were reviewed by two independent observers (Z.Z. and J.L.), according to the screening flow chart (Fig. 1). In the case of multiple studies from the same cohort, the most recent study was selected.

Intraoperative language mapping strategy

Four cohorts from the following four medical centres were included: (i) Montreal Neurological Institute (MNI), Canada, between 1946 and 1956[1]; (ii) Department of Neurological Surgery, University of California, San Francisco (UCSF), USA, between 1999 and 2014[3]; (iii) Gui de Chauliac Hospital (GCH), France, between 2004 and 2019[5]; and (iv) Huashan Hospital (HSH), China, between 2011 and 2018 (see the Supplementary material for subject information for HSH). All the included subjects had intraoperative DES language mapping under awake craniotomy.[1,3,5,7] Three stimulators were used for mapping in the MNI cohort,[1] including the thyratron stimulator, square wave generator, and Rahm stimulator. The three other centres used the paradigm of Ojemann stimulators (5-mm interval bipolar electrode, current-constant bipolar square wave, 1 ms wave width, and 60 Hz stimulation frequency).[3,6,7] The detailed strategies for determining the current intensity for each centre are presented in Table 1. The exposed cortex was stimulated at an interval of 1 cm, during which patients were instructed to perform number counting and picture naming tasks. The definitions of speech arrest and anomia are

```
┌──────────────────────────────┐        ┌──────────────────────────────┐
│ 743 Studies identified through│        │ 1 Additional study including  │
│    database searching         │        │  updated data from Huashan    │
│                               │        │         Hospital              │
└──────────────────────────────┘        └──────────────────────────────┘

              ┌──────────────────────────────┐
              │   744 Studies identified      │
              └──────────────────────────────┘

                                    ┌──────────────────────────────┐
                                    │ 236 Excluded duplicated Studies│
                                    └──────────────────────────────┘

              ┌──────────────────────────────┐
              │ 508 Studies after duplicates  │
              │          removed              │
              └──────────────────────────────┘

                                    ┌──────────────────────────────┐
                                    │ 418 Excluded by title and      │
                                    │  abstract for not DES study    │
                                    └──────────────────────────────┘

              ┌──────────────────────────────┐
              │ 90 Full-text studies assessed │
              │        for eligibility        │
              └──────────────────────────────┘

┌──────────────────────┐            ┌──────────────────────────────────────┐
│ 1 Additional study    │            │ 79 Excluded studies:                  │
│ from reference lists  │            │  Review                   (n=13)      │
└──────────────────────┘            │  Subcortical stimulation  (n=14)      │
                                    │  Not left lateral hemisphere (n=2)    │
                                    │  Not language mapping                 │
                                    │    (counting/naming)      (n=16)      │
                                    │  Fewer than 50 patients   (n=34)      │
                                    └──────────────────────────────────────┘

              ┌──────────────────────────────┐
              │     12 Candidate studies      │
              └──────────────────────────────┘

                                    ┌──────────────────────────────┐
                                    │ 8 Excluded studies:           │
                                    │  No positive coordinate data (n=3)│
                                    │  Same cohort          (n=5)   │
                                    └──────────────────────────────┘

              ┌──────────────────────────────┐
              │  4 Studies included for       │
              │    distribution analysis      │
              └──────────────────────────────┘
```
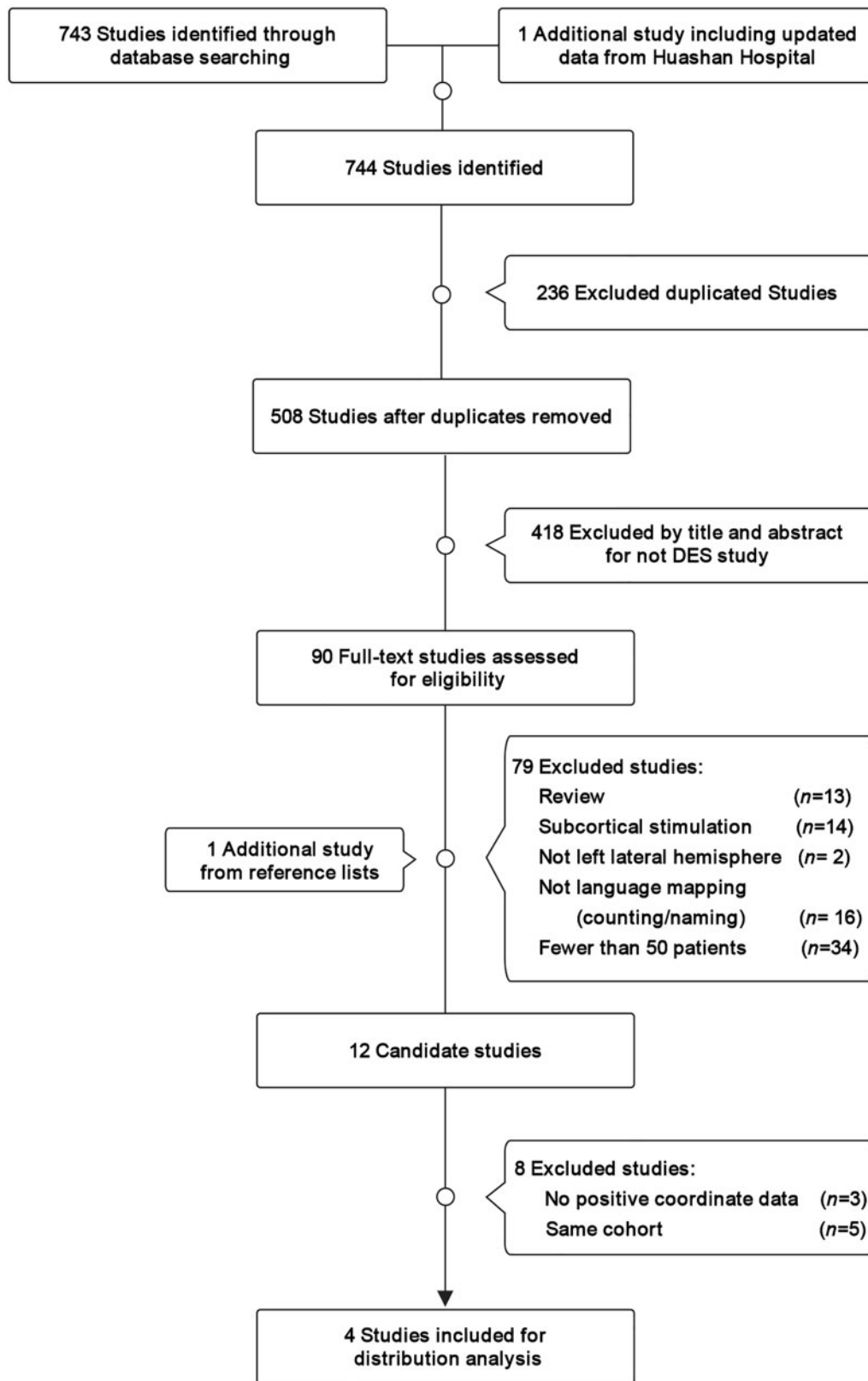
Figure 1 Flow chart for the literature screening.

described above and are shown schematically in Fig. 2A and B. Each site was discontinuously stimulated at least three times and was determined as a positive site when at least two of them induced language disturbances, without after-discharge or epileptic seizure. These positive sites were marked with sterile labels. The recording methods for these positive sites on the individual brain surface were as follows[1,3,6,7]: intraoperative photos with labels were taken by all four centres (Fig. 2C); neuro-

Table 1 Clinical characteristics of subjects and mapping strategies

	MNI	UCSF	GCH	HSH
Patients, n	110	102	256	256
Hemisphere, n (%)				
Left	90 (81.8)	98 (96.1)	155 (60.5)	255 (99.6)
Right	20 (18.2)	4 (3.9)	101 (39.5)	1 (0.4)
Language	Indo-European (mostly English and French)	Indo-European (mostly English)	Indo-European (mostly French)	Sino-Tibetan (Mandarin)
Disease	Mostly focal epilepsy	Tumour	Tumour	Tumour
WHO tumour grade, n(%)				
I or II	Not applicable	41 (40.2)	256 (100.0)	165 (64.5)
III	Not applicable	37 (36.3)	0 (0.0)	50 (19.5)
IV	Not applicable	24 (23.5)	0 (0.0)	41 (16.0)
Positive sites on the left hemisphere, n				
Speech arrest	219	75	198	425
Anomia	68	99	126	130
Stimulator	(i) Thyratron stimulator (before 1945) (ii) Rahm stimulator (1945–1951) (iii) Square wave generator (after 1951); (bipolar, mostly 60 Hz frequency)	Ojemann stimulator (5-mm interval bipolar electrodes, current-constant bipolar square wave, 1 ms wave width, 60 Hz frequency)		
Language mapping strategy	Stimulate the postcentral gyrus until sensory responses were induced (mostly 1–3 V). Language mapping voltage was set twice the voltage.	The after-discharge threshold was induced before mapping. The current intensity was set to the maximum intensity without after-discharges.	Stimulate the central lobe until reliable motor/sensory responses were induced. Language mapping current was set to the same intensity.	Stimulate the precentral gyrus until motor responses were induced. Language mapping current was set to the same intensity.
Stimulation intensity range	⩽8 mA	1–3.5 mA	2–4 mA	1–3 mA

navigation snapshots were recorded by USCF and HSH (Fig. 2D); and intraoperative hand-painted brain surfaces were recorded by MNI.[1]
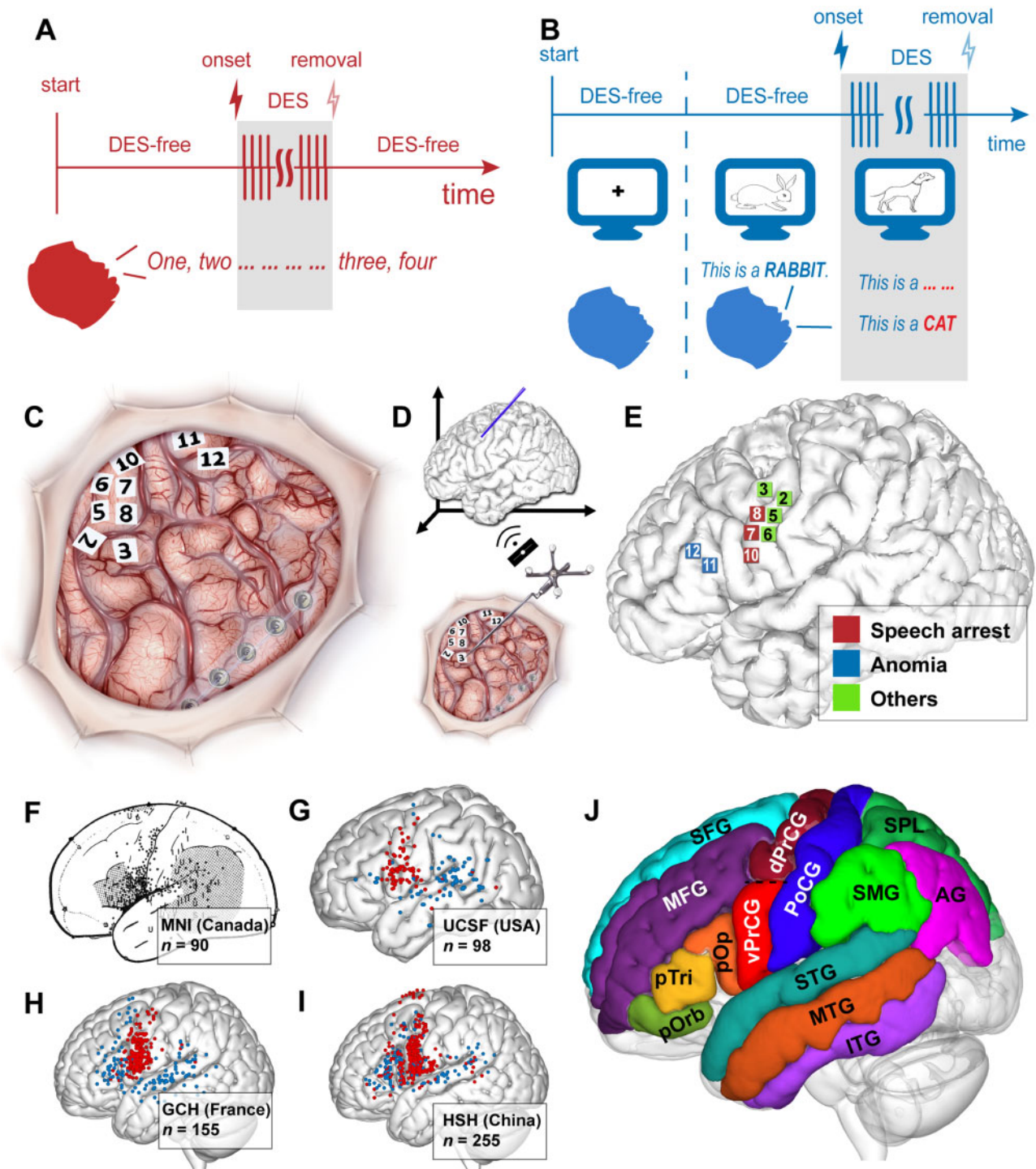
Normalization and generation of speech maps

The MNI 152 (2009, asymmetric) was chosen as the common standard template. To project all positive sites from different centres onto the same brain template, different techniques were used to obtain the coordinates of the standard space, according to the obtained data. Since the coordinates of the positive sites from the MNI centre were recorded on a hand-drawn brain template (Fig. 2F), these sites were plotted on the MNI 152 template using the MRICron software (https://www.nitrc.org/projects/mricron), according to the anatomical relationship between the sulci and gyri. An affine transformation was used to normalize the coordinates of the Colin 27 template from UCSF (Fig. 2G) to the MNI 152 template. This affine transformation matrix was built by the 'Old Normalise' Tool of SPM software (version 12), which described the spatial correspondence from the Colin 27 image to the MNI 152 template image. The positive sites of GCH and HSH were directly projected from individual brain surfaces onto the MNI 152 according to anatomical landmarks (Fig. 2H and I). All positive sites from the four centres were aligned to the pial surface of the MNI 152 template.[13] The anatomical classification of the positive sites was based on a standard atlas, the Desikan-Killiany Atlas.[14] Since the ventral part of the precentral gyrus is a hot language mapping region in the previous literature,[3,6,7] we used the z = 43 plane in MNI standard space (at the level of the intersection of the inferior frontal sulcus and the precentral sulcus) as the boundary to subdivide the precentral gyrus into ventral and dorsal portions (Fig. 2J). To compare the distribution patterns of language sites across the four medical centres, the percentages of language sites in different regions were separately calculated and tested between medical centres using Spearman's correlation analysis. To assess the distribution of positive sites, a kernel density estimation (KDE) was then performed.[15] Taking into account the uncertainty caused by the spatial resolution (1 cm × 1 cm),[16] all positive sites were smoothed using Gaussian smoothing, with 10-mm full-width at half-maximum, which were merged to build the density map. Additionally, to reduce the potential bias caused by the number of times of stimulation across the different regions, the probabilistic maps of speech arrest and anomia were also generated, based on available data obtained from MNI, UCSF, and HSH (Supplementary material).

Cluster analysis and permutation test

Cluster analysis was conducted using R Project to evaluate the group-level distribution pattern of the functional sites. Initially, the Duda-Hart test[17] was performed to determine whether each set of positive sites should be divided into two or more clusters. Merely those with Duda-Hart statistics > 1.645 (P < 0.05) were further analysed using cluster analysis, while those with Duda-Hart statistics < 1.645 were considered as a single cluster. Sites with less than eight adjacent points (an average of two points per centre) in the 10-mm range were considered outliers and excluded. The remaining points were then subjected to hierarchical cluster analysis.[18] The cluster number was iterated from 2 to 10, where the one with the highest silhouette score[19] was selected as the optimal number. Finally, the speech arrest sites were grouped into four clusters, while the anomia sites

Figure 2 The technical route of acquisition and normalization of the language sites. (**A** and **B**) Sketch maps for the number counting task (red timeline) and picture naming task (blue timeline). (**A**) Speech arrest (marked in grey) is defined as the DES-induced complete interruption while counting, without obvious oral, facial, mandibular, and laryngeal muscle movement. (**B**) Anomia (marked in grey) is defined as the DES-induced inability to name the object in a picture, or misnaming by using the wrong word (e.g. using 'cat' instead of 'dog'), while still being able to speak the leading word [e.g. 'This is a(n) …']. (**C–E**) Intraoperative photographs with sterile labels to mark the positive sites (**C**) and/or neuro-navigation images (**D**) were used to record the locations of these sites on the individual surfaces (**E**). (**F–I**) The original functional maps from the four centres were projected onto different templates. These include (**F**) the line graph template of MNI, (**G**) Colin 27 template of UCSF, and MNI 152 template of (**H**) GCH and (**I**) HSH. (**J**) All positive sites were normalized to the common MNI 152 template. AG = angular gyrus; dPrCG = dorsal precentral gyrus; ITG = inferior temporal gyrus; MFG = middle frontal gyrus; MTG = middle temporal gyrus; PoCG = postcentral gyrus; pOrb = pars orbitalis; SFG = superior frontal gyrus; SMG = supramarginal gyrus; SPL = superior parietal lobule.

were grouped into two clusters. The characteristics of these clusters were statistically described as centroid ± standard deviation (SD).

Since there was spatial overlapping between the speech arrest and anomia maps, in both the lateral frontal cortex and superior temporal gyrus (STG), a permutation test[20] was performed to

determine whether the overlapped clusters of two different disruptions had the same spatial distribution (Supplementary material). The Euclidean distance between the centroids (ECD) of the two clusters was calculated. A P-value of <0.05 indicated significant differences between clusters.

Comparison with functional MRI datasets

To clarify whether our DES results are comparable to the functional MRI datasets, we constructed the resting-state functional connectivity maps from Wu-Min Human Connectome Project (HCP) Data dataset (see Supplementary material and Supplementary Figs 1 and 2 for detailed methods and results).

Data availability

Data involved in this study are available upon reasonable request.

Results

In the present study, 598 subjects were included to generate functional maps. Three different languages are spoken, with 90 subjects from MNI in Canada, mostly speaking English or French; 98 subjects from UCSF in the USA, mostly speaking English; 155 subjects from GCH in France, mostly speaking French; and 255 subjects from HSH in China, mostly speaking Mandarin. Detailed clinical characteristics of these subjects and the stimulation strategy of each centre are presented in Table 1.

Spatial distribution of speech arrest sites

A total of 917 speech arrest sites (219 sites from MNI; 75 sites from UCSF; 198 sites from GCH; and 425 sites from HSH) were included (Fig. 3A–E and Supplementary Table 4), with overlap across different centres. A Spearman's correlation analysis showed that speech arrest sites had similar patterns across the four centres and the pair-wise correlation coefficients ranged from 0.6 to 0.85 ($P < 0.05$) (Fig. 3H and I). After combining all the sites from different centres, the peak of the speech arrest was found to be localized to the ventral part of the precentral gyrus (vPrCG) (–66, 4, 17) (Fig. 3E, F and J), not the 'classic' Broca's area (pOp, pars opercularis; pTri, pars triangularis). Furthermore, the hierarchical clustering analysis revealed that all the speech arrest sites could be divided into four clusters (Fig. 3G and Supplementary Fig. 4A). The anterior cluster was the largest (cluster 1, Fig. 3G), containing 597 sites (accounting for 65.1% of the total speech arrest sites). Its centroid was located in the vPrCG, which mainly covered the ventral portion of the central lobe and pOp. The middle cluster (cluster 2) contained 203 sites (22.1%), which were superiorly centred in the vPrCG, while also covering the dorsal precentral gyrus and posterior middle frontal gyrus. The superior cluster (cluster 3, Fig. 3G) contained 30 sites (3.2%) in the supplementary motor area. The posterior cluster (cluster 4, Fig. 3G) contained 41 sites (4.4%), which was centred in the posterior part of the STG (pSTG), just inferior to the Sylvian fissure. This cluster mainly covered the cerebral regions around the posterior Sylvian fissure, which included the pSTG and supramarginal gyrus. The coordinates of the centroids and peak points for each cluster were illustrated in Supplementary Table 1. Also, the probabilistic map showed a similar distribution pattern to the KDE analysis (Supplementary Fig. 3A and D).

Spatial distribution of anomia sites

A total of 423 anomia sites from four centres (68 sites from MNI; 99 sites from UCSF; 126 sites from GCH; and 130 sites from HSH) were included for further analysis (Fig. 4A–E and Supplementary Table 5). They were mainly distributed in the inferior frontal gyrus and posterior temporal lobe. The Spearman's correlations showed that there was significant consistency ($r = 0.81$, $P = 0.0039$) between the two centres with the most sites (HSH and GCH), as well as between GCH and UCSF ($r = 0.60$, $P = 0.022$) (Fig. 4H and I). As the sites reported by any single centre were limited and sparse, extracting the peak coordinate and centroid would be unreliable. The combined results showed a more straightforward pattern at the inferior frontal gyrus and STG (Fig. 4E). The KDE analysis revealed two peaks: One peak at (–70, –34, 11) in the posterior part of the STG, with a maximum density of 0.052, and another peak at (–62, 22, 11) in the pTri, with a maximum density of 0.056 (Fig. 4F and J). Besides, the probabilistic map based on the stimulation times also presented a similar distribution pattern as the KDE analysis (Supplementary Fig. 3B and E). These anomia sites can be divided into two clusters through hierarchical clustering analysis (Fig. 4G and Supplementary Fig. 4B). The posterior cluster (cluster 1, Fig. 4G) consisted of 194 sites (accounting for 45.9% of the total anomia sites), and its centroid was located in the pSTG. This cluster covered the pSTG and middle temporal gyrus, as well as the inferior portions of the supramarginal gyrus. Cluster 2 consisted of 158 sites (37.4%), which centred at the pTri. This cluster mainly contained sites from the pOp, pTri, and posterior middle frontal gyrus. The coordinates of the centroids and peak points for each cluster are illustrated in Supplementary Table 2.

## The spatial relationship between speech arrest and anomia sites

Since speech arrest and anomia sites appeared to partially overlap in the inferior frontal lobe and pSTG (Fig. 5A and Supplementary Fig. 3C), a permutation test was performed to test the spatial discrepancy. The permutation test revealed that the anomia cluster was significantly more anterior than the speech arrest cluster in the lateral frontal cortex (ECD = 16.6 mm, $P < 0.001$). For the pSTG, the anomia cluster was significantly more anterior and inferior than the speech arrest sites (ECD = 11.8 mm, $P < 0.001$) (Fig. 5B).

To evaluate the distribution of speech arrest and anomia in each cerebral region, the percentage (% of all language sites) of these two responses were calculated and tested using either the chi-square or Fisher's exact probability test. It was found that more speech arrest responses were induced in the central lobe ($P < 0.001$), pOp ($P = 0.001$), and superior frontal gyrus ($P < 0.001$), compared to anomia. More anomia responses were induced in the pTri ($P = 0.007$), STG ($P < 0.001$), and middle temporal gyrus ($P < 0.001$) (Fig. 5C).

Subgroup analysis

Compared with the other three series, the data from MNI was heterogeneous in terms of electrical stimulators, stimulation strategies, brain templates for recording the stimulation sites, and disease types of subjects (Table 1). Therefore, we performed a subgroup analysis by excluding the MNI data and reanalysing the distribution of the positive sites from HSH, GCH and UCSF (Figs 6A and 7A).

In terms of speech arrest, the data of HSH, GCH and UCSF consistently showed the absolute dominant distribution of speech arrest sites in vPrCG (Fig. 6D and E). Cluster analysis only revealed two clusters. The ventral cluster (cluster II, Fig. 6C) contained 496 (71.1%) sites, the centroid of which was located in the vPrCG. The dorsal cluster (cluster I, Fig. 6C) contained 180 (25.8%) sites, which also centroided in the vPrCG. The centroids of these two clusters
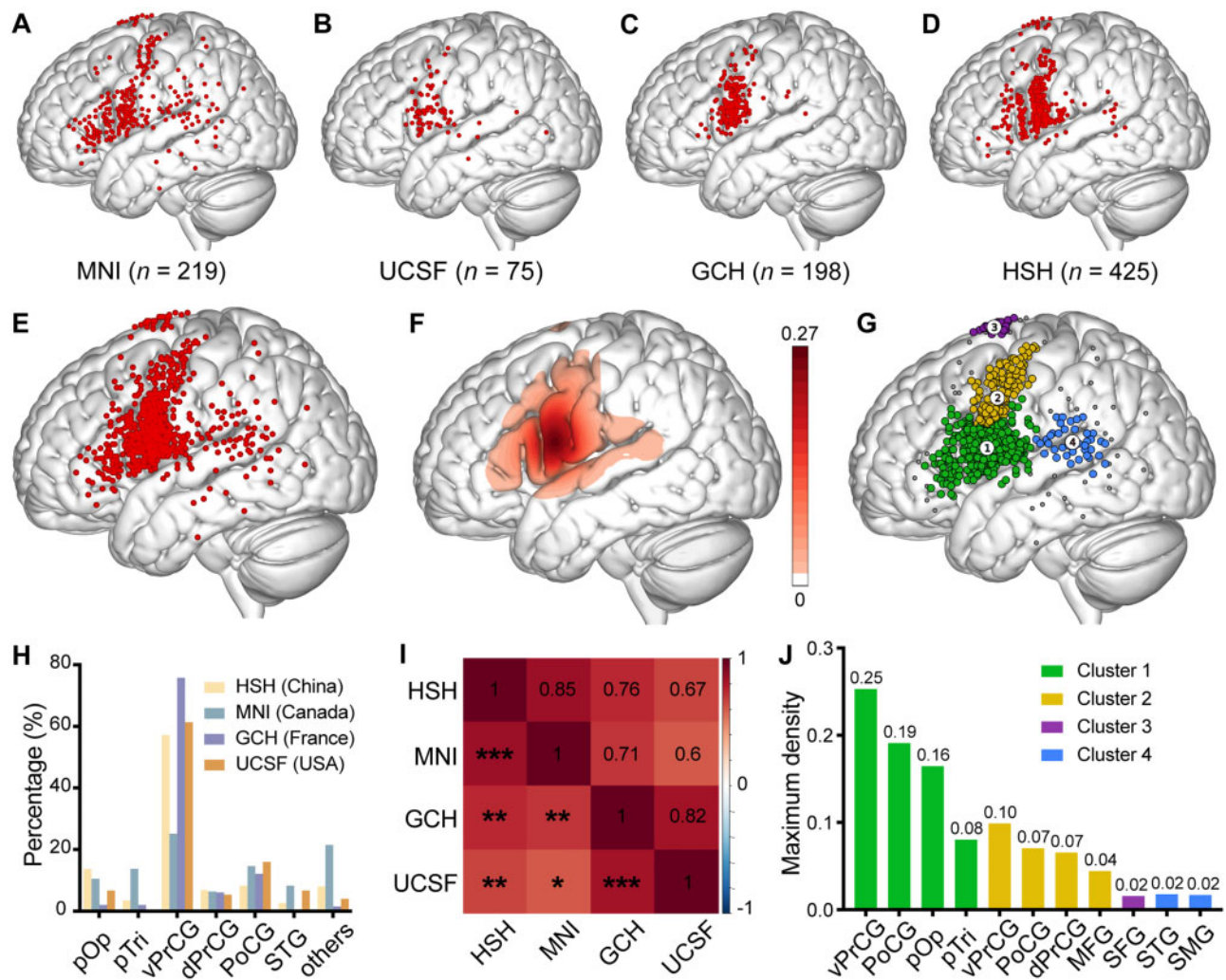
Figure 3 Spatial distribution of the speech arrest sites. (**A–E**) The speech arrest sites (red) from (**A**) MNI, (**B**) UCSF, (**C**) GCH, and (**D**) HSHwere separately plotted on the same brain template (MNI 152 template). (**E**) A total of 917 speech arrest sites from the four centres were gathered on the same template. (**F**) The density map of the speech arrest sites shows that they peaked in the vPrCG. (**G**) The speech arrest sites were split into four clusters (coloured by cluster labels) after eliminating outlier (grey), with the centroids marked with circled numbers of the cluster labels. (**H**) The percentage of speech arrest sites in the different regions, across the four medical centres, are shown. (**I**) The heat map shows the correlations of spatial distributions between different medical centres. The numbers indicate the Spearman's correlation coefficients, while the labels indicate the significance of the correlations (*$P < 0.05$; **$P < 0.01$; ***$P < 0.001$). (**J**) The maximum density of the major regions in each cluster are shown (coloured by cluster labels). dPrCG = dorsal precentral gyrus; MFG = middle frontal gyrus; PoCG = postcentral gyrus; SFG = superior frontal gyrus; SMG = supramarginal gyrus.

were similar to those of the two largest clusters (cluster 1 and 2, Fig. 3G) based on all four datasets. However, the original SMA cluster and the posterior peri-Sylvian cluster (clusters 3 and 4, Fig. 3G) failed to form discrete clusters due to insufficient density. The density map showed that the peak of speech arrest was located at (–66, 4, 17) in the ventral premotor cortex within cluster II (Fig. 6B and F).

For anomia, the data form UCSF, GCH and HSH showed even more consistency after removing MNI data ($r = 0.81$, $P < 0.001$ between GCH and HSH; $r = 0.60$, $P < 0.05$ between GCH and UCSF; $r = 0.44$, $P = 0.11$ between HSH and UCSF) (Fig. 7D and E). Furthermore, cluster analysis also showed two clusters similar to those reported from the four datasets (cluster 1 and 2, Fig. 4G). The anterior cluster (cluster II, Fig. 7C) consisted of 127 (35.8%) sites with a centroid in pTri, peaked at (–60, 24, 11) (Fig. 7B and F). The posterior cluster (cluster I, Fig. 7C) had 186 (52.4%) sites, which centred in pSTG and peaked at (–70, –32, 11) (Fig. 7B and F).

Discussion

Comparison of the language cortex distributions across languages

Our results showed a similar distribution of speech arrest and anomia among English, French, and Mandarin (Figs 3I and 4I), which indicates that different languages might share a similar neural basis of speech motor control/output and lexical access/semantics. Despite the cross-continental differences presented in this study, humans generally use similar brain regions to process speech output/speech motor control or lexical retrieval/semantics while learning different languages (alphabetic or ideographic languages) and phonemic structures. Although not surprising, it provides essential causal evidence across English, French, and Mandarin, for 'the minimal common language network'.[21,22] In addition, there were still some subtle differences. For example, more speech arrest sites from HSH (Mandarin-speaking) and MNI (English or
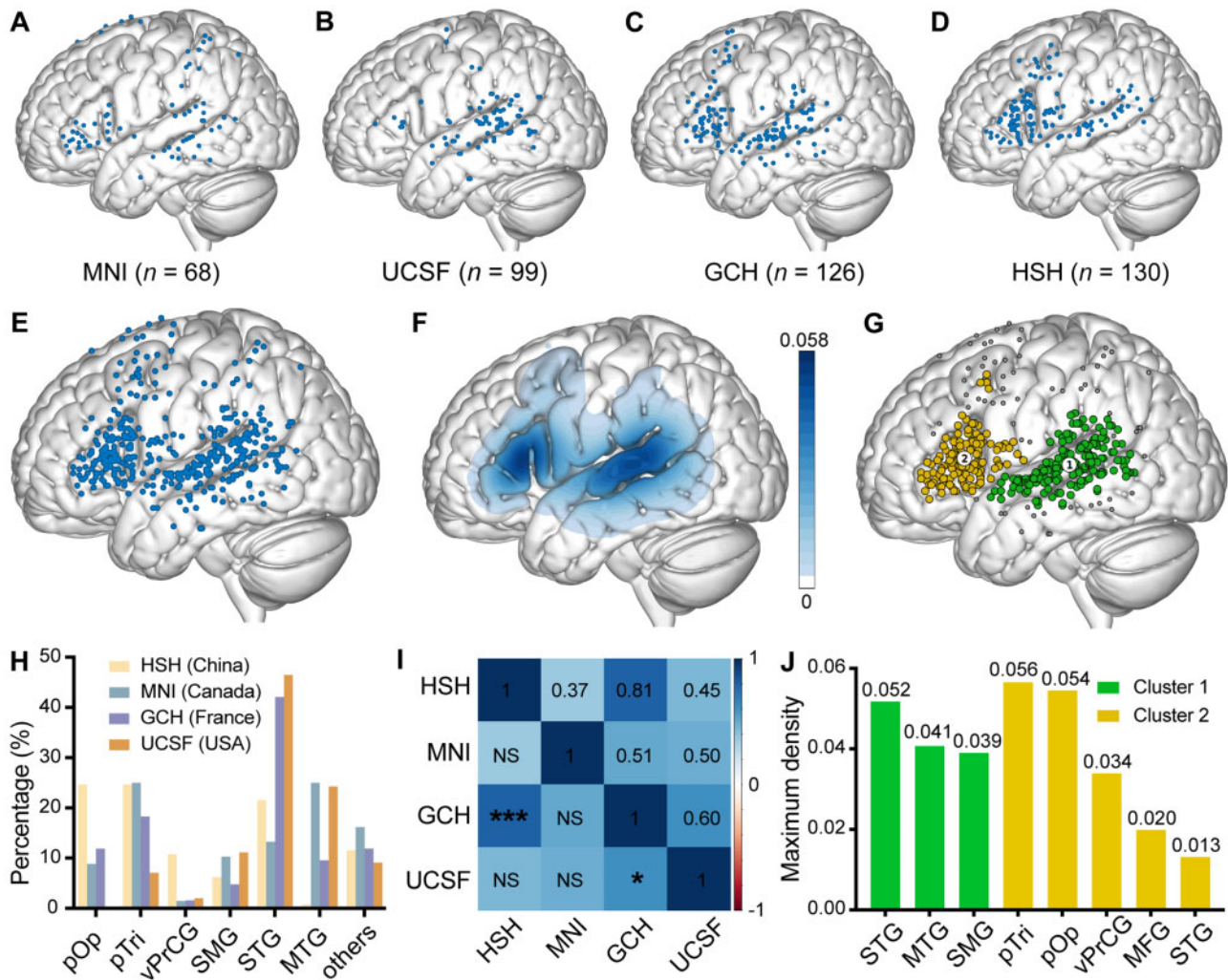
Figure 4 Spatial distribution of anomia sites. (**A–E**) Anomia sites (blue) from (**A**) MNI, (**B**) UCSF, (**C**) GCH and (**D**) HSH were separately plotted on the same brain template (MNI 152 template). (**E**) A total of 423 anomia sites from the four centres were gathered on the same template. (**F**) The density map of the anomia sites is shown. (**G**) The cluster analysis revealed that the anomia sites could be divided into two clusters (coloured by cluster labels) after eliminating outlier (grey), with the centroids marked with circled numbers of the cluster labels. (**H**) The percentage of anomia sites in the different regions across the four medical centres is shown. (**I**) The heat map shows the correlations between different medical centres. The numbers indicate the Spearman's correlation coefficients, while the labels indicate the significance of the correlations (*$P < 0.05$; ***$P < 0.001$; NS = non-significant). (**J**) The maximum density of the major regions in each cluster (coloured by cluster label). MFG = middle frontal gyrus; MTG = middle temporal gyrus; SMG = supramarginal gyrus.

French) were elicited than UCSF and GCH in the pOp and posterior middle frontal gyrus, which is consistent with the previous study.[7,23] This discrepancy might be explained by a higher stimulation intensity in the MNI centre, which may lead to a greater probability of the local spread of current and the remote effect via white matter pathway.[11] Another interpretation is that Mandarin involves more orthography-to-phonology conversion in the posterior middle frontal gyrus, compared to alphabetic languages.[24] As for anomia, significant correlations between GCH and HSH, and between GCH and UCSF were found, suggesting that they had similar distributions. At the same time, other pairwise comparisons were not significantly correlated. A possible explanation of why MNI was poorly correlated with others could be that there were more extensive cortex exposures and a higher stimulation intensity for epilepsy surgeries in MNI, which induced more sites at the parietal lobe. After excluding the most heterogeneous data from MNI centre, the subgroup analysis showed more consistent bimodal pattern with the pTri and the pSTG as two discrete peaks of anomia. Based on these findings, it can be inferred that different languages share the same distribution pattern of anomia.

Spatial distribution and underlying connectivity of speech arrest

We found the largest cluster of speech arrest was situated in a broader area of the lateral frontal cortex, which included the vPrCG, pOp, and pTri. However, the centroid and coordinate of maximum density were in the vPrCG, instead of the 'classic' Broca's area (pOp and pTri). This finding is consistent with previous studies, which demonstrated that the ventral premotor cortex is the epicenter of stimulation-induced speech arrest.[6,7] This area was posited as a 'speech sound map' or 'syllabary' in speech production models. It might contain motor programmes that are probably involved in the motor programming stage of speech production.[25,26] However, a recent study found stimulating some speech arrest sites in vPrCG also elicited the arrest of ongoing manual movements (negative motor responses).[27] It might suggest
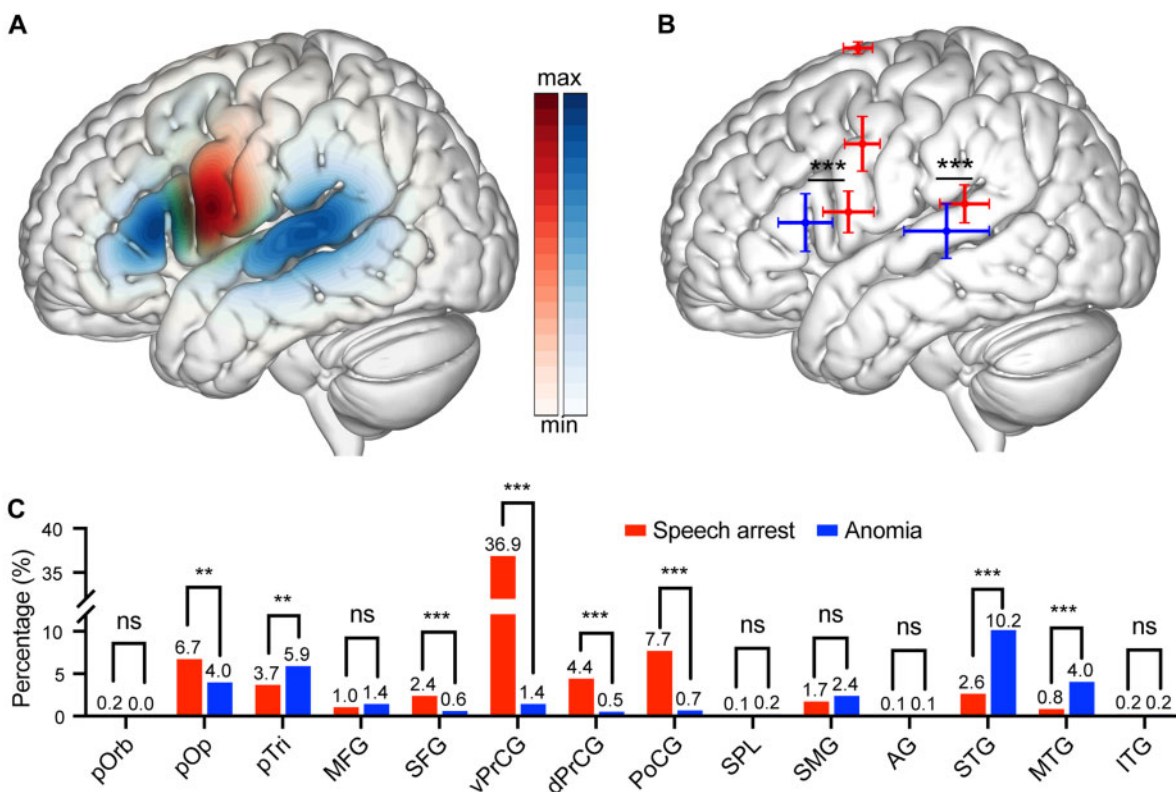
Figure 5 Spatial relationship between speech arrest and the anomia sites. (**A**) The merged image for the speech arrest and anomia density maps is shown. (**B**) The merged cluster map for the speech arrest (red) and anomia (blue) sites is shown (plotted as centroid ± SD in the y-z-axes of MNI space). (**C**) The percentages (% of total language sites) for speech arrest and anomia in each cerebral region. **$P < 0.01$; ***$P < 0.001$; ns = not significantly different. AG = angular gyrus; dPrCG = dorsal precentral gyrus; ITG = inferior temporal gyrus; MFG = middle frontal gyrus; MTG = middle temporal gyrus; PoCG = postcentral gyrus; pOrb = pars orbitalis; SFG = superior frontal gyrus; SMG = supramarginal gyrus; SPL = superior parietal lobule.
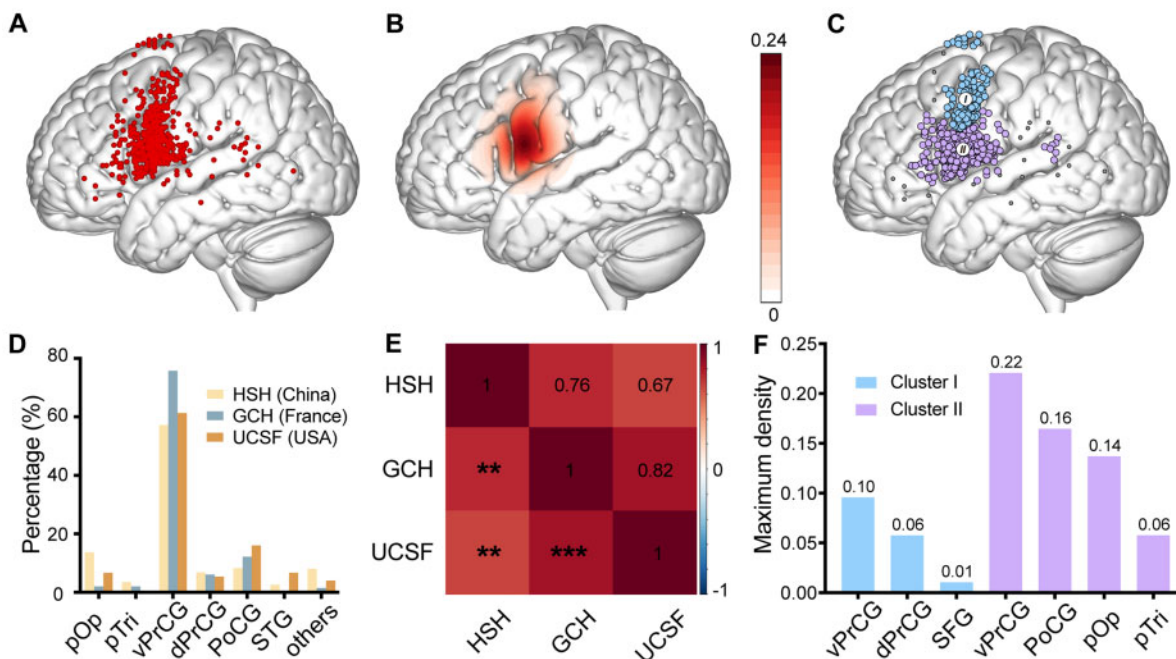
Figure 6 Subgroup analysis of the speech arrest sites. (**A**) A total of 698 speech arrest sites (red) from HSH, GCH and UCSF were pooled together on MNI 152 template. (**B**) The density map of the speech arrest sites showed that they peaked in the vPrCG. (**C**) The speech arrest sites were split into two clusters (coloured by cluster labels) after eliminating outlier (grey), with the centroids marked with circled Roman numerals of the cluster labels. (**D**) The percentage of speech arrest sites in the different regions, across the three medical centres, are shown. (**E**) The heat map shows the correlations of spatial distributions between different medical centres. The numbers indicate the Spearman's correlation coefficients, while the labels indicate the significance of the correlations (**$P < 0.01$; ***$P < 0.001$). (**F**) The maximum density of the major regions in each cluster are shown (coloured by cluster labels). dPrCG = dorsal precentral gyrus; PoCG = postcentral gyrus; pOrb = pars orbitalis; SFG = superior frontal gyrus; SMG = supramarginal gyrus.
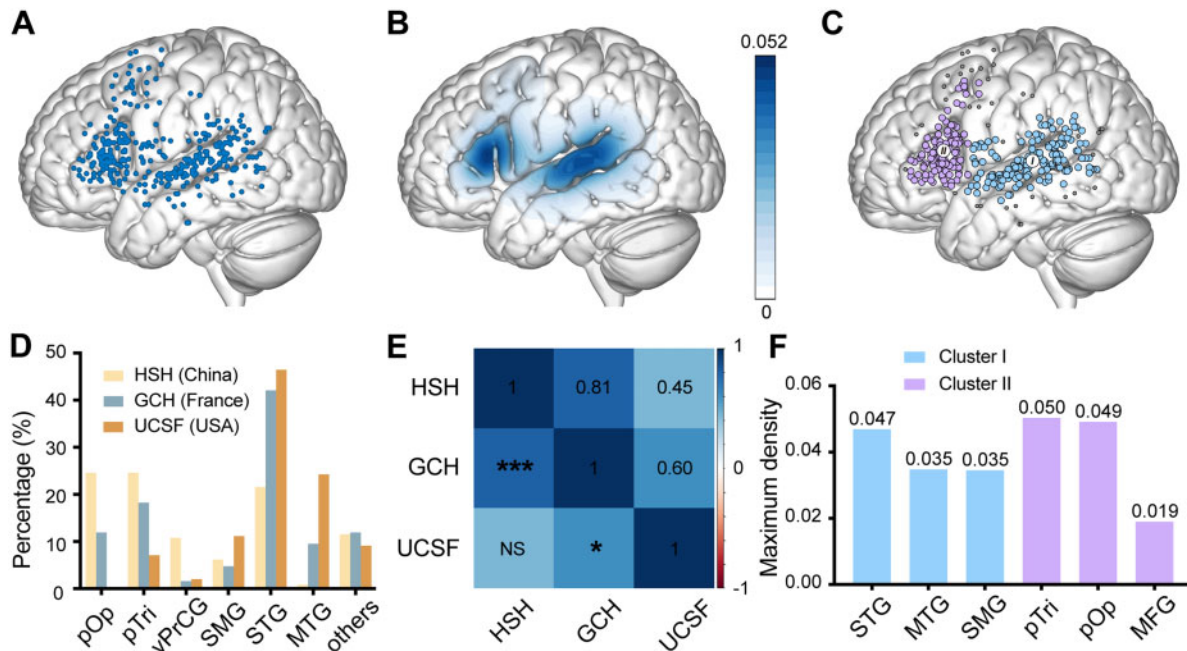
Figure 7 Subgroup analysis of the anomia sites. (**A**) A total of 355 anomia sites (blue) from HSH, GCH and UCSF were pooled together on MNI 152 template. (**B**) The density map of the anomia sites showed that they peaked in the pTr and pSTG. (**C**) The anomia sites were split into two clusters (coloured by cluster labels) after eliminating outlier (grey), with the centroids marked with circled Roman numerals of the cluster labels. (**D**) The percentage of anomia sites in the different regions, across the three medical centres, are shown. (**E**) The heat map shows the correlations of spatial distributions between different medical centres. The numbers indicate the Spearman's correlation coefficients, while the labels indicate the significance of the correlations (*P < 0.05; ***P < 0.001; NS = non-significant). (**F**) The maximum density of the major regions in each cluster are shown (coloured by cluster labels). MFG = middle frontal gyrus; MTG = middle temporal gyrus; SMG = supramarginal gyrus.

that speech arrest sites in the lateral frontal cortex could be categorized into two different groups (speech-specific sites and general negative motor response sites).[28,29]

Another cluster was identified in the dorsal precentral gyrus and posterior middle frontal gyrus at the vertical level of the middle frontal gyrus. In addition to the potential interpretation as negative motor areas, the cluster is also spatially similar to the re-emerged cortical area 55b.[28–30] Structurally, area 55 b is isolated from the surrounding cortex, according to the gradients of the myelin content. Functionally, this is universally activated in both covert speech production and listening tasks.[28,30,31] Furthermore, the resection of this area resulted in pure apraxia of speech (a disorder of the articulatory coordination and planning in speech sound production, leading to deficits in articulation, prosody, and fluency), which also explains the DES-induced speech arrest response in this region.[28,32]

Furthermore, an isolated cluster was identified in the SMA. This area was posited as an 'initial map' in speech production models and is involved in the initiation and coordination of speech production.[25] Diffusion tensor imaging studies show that the SMA is connected to the ventral premotor area and pOp via the frontal aslant tract (FAT), and DES of this bundle induces speech arrest.[33–35] Most importantly, besides the frontal regions, speech arrest was also elicited in the Wernicke area of the pSTG, which is approximately centred in the Sylvian-parietal-temporal area. However, previous studies largely overlooked this area as a speech production centre, due to a low positive rate and relatively fewer chances of exposure during surgeries. The Sylvian-parietal-temporal area was assumed to subserve the transformation between auditory or visual information, and articulatory representations of speech, according to the dual-stream model proposed by Hickok and Poeppel.[36]

Moreover, the evidence obtained from fibre tractography was also in line with the present findings. The inferior and middle

clusters of the frontal lobe and the pSTG cluster overlapped with the terminations of the superior longitudinal fasciculus-III (SLF-III)/arcuate fasciculus (AF).[37–39] The DES of the SLF-III was found to induce anarthria or speech arrest, while the DES of the AF induced phonemic paraphasia,[37] providing subcortical connective evidence.[37,40] It should be noted that the components of SMA and pSTG clusters mainly came from MNI, so that in the subgroup analysis, the speech arrest sites from the other three centres were too sparse to form these two clusters. One possible explanation of the sites in these two clusters might be due to the remote effects via subcortical fibres caused by the excessive current intensity.[41] However, even if SMA and pSTG clusters were caused by remote effects,[41] the positive sites induced in these regions might still be essential for speech production because it indicated they were the cortical regions of the dorsal phonological streams (pSTG by SLF-III/AF, and SMA by FAT).

Spatial distribution and underlying connectivity of anomia

It was found that anomia sites can be split into two clusters with equivalent density. The finding that the pTri is the frontal epicentre of lexical-semantic processing is consistent with neuroimaging[42] and DES studies.[43] In addition, our results reported a gradual transitional pattern from speech output function to a higher-level lexical/semantic processing aspect in the direction from ventral premotor cortex to the pTri of Broca's area (Fig. 5A). This pattern fits well to the modern understanding of the multi-receptor and co-activation based parcellation of the anterior language region, where the caudal part of the Broca's area (pOp) and the ventral premotor cortex have predominantly motor functions, while the rostral part of the Broca's area (predominantly pTri) have more prefrontal functions.[44,45] Concerning the role of the pOp, this

has been contentious for several decades. Although the present data suggest that the pOp is implicated in both lexical retrieval (eliciting anomia) and speech output (eliciting speech arrest), converging evidence from DES and neuroimaging studies have also revealed that syntactic processing is subserved specifically by the pOp, at the level of sentence production and comprehension.[46–50] Thus, more intraoperative tasks including counting, naming and sentence production/comprehension might be required during mapping the function of pOp.

In addition to the frontal epicentre, it is not surprising that the posterior cluster was located in the 'classic' Wernicke's area, which also expanded to the mid-posterior STG and middle temporal gyrus, and inferior supramarginal gyrus, with the centroid and peak point located in the pSTG. Activation of the mid-posterior STG in semantic processing has been supported by multiple functional MRI studies, which utilized auditory and visual naming tasks among healthy volunteers.[51–53] From the perspective of fibre connectivity, these two clusters overlapped with the frontal and temporal terminations of the inferior fronto-occipital fasciculus,[54–56] respectively. This location is an important part of the ventral semantic stream. Stimulation to this bundle can elicit semantic paraphasia,[57,58] further supporting our findings.

Limitations

Our study had some limitations. First, because of the lack of large sample studies on the right hemisphere, only data on the left hemisphere was included. Therefore, we were unable to compare the relationship of language distribution between the two hemispheres. Second, the numbers of stimulations in each brain region were highly variable; that is, the exposure of the cortex was unbalanced. Hence, the distribution of the speech disturbance sites was likely biased. However, the available probability maps from the three medical centres demonstrated similar distribution patterns (Supplementary Fig. 3). There is thus reason to suggest that these maps represent ground truth that the vPrCG is the most critical cortical region of the minimal common network of speech output, while the pTri and pSTG are those of the semantic/lexical processing. Third, the subject's handedness information is not fully available (see 'Handedness information' in the Supplementary material). However, we do not think handedness would significantly affect our results. In most people, the left hemisphere of the brain is dominant for language, irrespective of the handedness.[1,59,60] Besides, the previous direct electrical cortical stimulation study showed that data in the left hemispheres of left-handed/ambidextrous patients suggested an analogous pattern of speech output and naming to right-handed patients.[6] Finally, we only focused on the consistency of the language cortex of cross-lingual spoken language, and the possible discrepancy between spoken and non-spoken language was not covered. Interestingly, a recent electrocorticography study showed that the cerebral regions for non-spoken sign language might differ from those of monolingual spoken language in terms of language production.[61]

Conclusion

This is by far the first multicentre DES language mapping study with the largest sample size. We highlighted the critical role of ventral precentral gyrus in the speech circuit, which challenged the dogmatic localizationist view (i.e. pOp/pTri are the speech output centre). We also highlighted two distinct functional peaks in pSTG and pTri, respectively, during semantic/lexical processing. The patterns of language maps were consistent across the three languages and provided evidence for common networks across languages, in the context of both speech and naming circuit. These

data can not only offer clinical neurologists and neurologic surgeons high-level, evidence-based guidelines for the definition of functional boundaries of language, but also provide better insight into fundamental language organization.

Competing interests

The authors report no competing interests.

Supplementary material

Supplementary material is available at *Brain* online.

References

1. Penfield W, Roberts L. Speech and brain mechanisms. Princeton University Press; 1959.
2. Ojemann G, Ojemann J, Lettich E, Berger M. Cortical language localization in left, dominant hemisphere. An electrical stimulation mapping investigation in 117 patients. *J Neurosurg*. 1989; 71(3):316–326.
3. Chang EF, Breshears JD, Raygor KP, Lau D, Molinaro AM, Berger MS. Stereotactic probability and variability of speech arrest and anomia sites during stimulation mapping of the language dominant hemisphere. *J Neurosurg*. 2017;126(1):114–121.
4. Sanai N, Mirzadeh Z, Berger MS. Functional outcome after language mapping for glioma resection. *N Engl J Med*. 2008;358(1): 18–27.
5. Sarubbo S, Tate M, De Benedictis A, et al. Mapping critical cortical hubs and white matter pathways by direct electrical stimulation: An original functional atlas of the human brain. *Neuroimage*. 2020;205:116237.
6. Tate MC, Herbet G, Moritz-Gasser S, Tate JE, Duffau H. Probabilistic map of critical functional regions of the human cerebral cortex: Broca's area revisited. *Brain*. 2014;137(Pt 10): 2773–2782.
7. Wu J, Lu J, Zhang H, et al. Direct evidence from intraoperative electrocortical stimulation indicates shared and distinct speech production center between Chinese and English languages. *Hum Brain Mapp*. 2015;36(12):4972–4985.
8. De Witt Hamer PC, Robles SG, Zwinderman AH, Duffau H, Berger MS. Impact of intraoperative stimulation brain mapping on glioma surgery outcome: A meta-analysis. *J Clin Oncol*. 2012; 30(20):2559–2565.
9. Müller DMJ, Robe PAJT, Eijgelaar RS, et al. Comparing glioblastoma surgery decisions between teams using brain maps of

tumor locations, biopsies, and resections. *JCO Clin Cancer Inform.* 2019;3:1–12.

10. Pallud J, Rigaux-Viode O, Corns R, et al. Direct electrical bipolar electrostimulation for functional cortical and subcortical cerebral mapping in awake craniotomy. Practical considerations. *Neurochirurgie.* 2017;63(3):164–174.

11. Borchers S, Himmelbach M, Logothetis N, Karnath HO. Direct electrical stimulation of human cortex - the gold standard for mapping brain functions? *Nat Rev Neurosci.* 2011;13(1):63–70.

12. Yuan B, Zhang N, Yan J, Cheng J, Lu J, Wu J. Tumor grade-related language and control network reorganization in patients with left cerebral glioma. *Cortex.* 2020;129:141–157.

13. Hamilton LS, Chang DL, Lee MB, Chang EF. Semi-automated anatomical labeling and inter-subject warping of high-density intracranial recording electrodes in electrocorticography. *Front Neuroinform.* 2017;11:62.

14. Desikan RS, Segonne F, Fischl B, et al. An automated labeling system for subdividing the human cerebral cortex on MRI scans into gyral based regions of interest. *NeuroImage.* 2006;31(3): 968–980.

15. Eickhoff SB, Laird AR, Grefkes C, Wang LE, Zilles K, Fox PT. Coordinate-based activation likelihood estimation meta-analysis of neuroimaging data: A random-effects approach based on empirical estimates of spatial uncertainty. *Hum Brain Mapp.* 2009;30(9):2907–2926.

16. Szelenyi A, Bello L, Duffau H, et al.; Workgroup for Intraoperative Management in Low-Grade Glioma Surgery within the European Low-Grade Glioma Network. Intraoperative electrical stimulation in awake craniotomy: Methodological aspects of current practice. *Neurosurg Focus.* 2010;28(2):E7.

17. Murtagh F, Farid MM. Pattern classification, by Richard O. Duda, Peter E. Hart, and David G. *Stork.* 2001;18(2):273–275.

18. Kisilevich S, Mansmann F, Nanni M, Rinzivillo S, Clustering S-T. Data mining and knowledge discovery handbook. Boston, MA: Springer US; 2010.

19. Rousseeuw PJ. Silhouettes: A graphical aid to the interpretation and validation of cluster analysis. *J Comput Appl Math.* 1987;20: 53–65.

20. Good PI. Permutation, parametric, and bootstrap tests of hypotheses. Springer Science & Business Media; 2006.

21. Brouwer H, Hoeks JC. A time and place for language comprehension: Mapping the N400 and the P600 to a minimal cortical network. *Front Hum Neurosci.* 2013;7:758.

22. Ius T, Angelini E, de Schotten MT, Mandonnet E, Duffau H. Evidence for potentials and limitations of brain plasticity using an atlas of functional resectability of WHO grade II gliomas: Towards a "minimal common brain". *NeuroImage.* 2011;56(3):992–1000.

23. Wu J, Lu J, Zhang H, Zhang J, Mao Y, Zhou L. Probabilistic map of language regions: Challenge and implication. *Brain.* 2015;138(Pt 3):e337.

24. Tan LH, Laird AR, Li K, Fox PT. Neuroanatomical correlates of phonological processing of Chinese characters and alphabetic words: A meta-analysis. *Hum Brain Mapping.* 2005;25(1):83–91.

25. Guenther FH. Neural control of speech. Mit Press; 2016.

26. Indefrey P. The spatial and temporal signatures of word production components: A critical update. *Front Psychol.* 2011;2:255.

27. Breshears JD, Southwell DG, Chang EF. Inhibition of manual movements at speech arrest sites in the posterior inferior frontal lobe. *Neurosurgery.* 2019;85(3):e496–e501.

28. Chang EF, Kurteff G, Andrews JP, et al. Pure apraxia of speech after resection based in the posterior middle frontal gyrus. *Neurosurgery.* 2020;87(3):E383–E389.

29. Rech F, Herbet G, Gaudeau Y, et al. A probabilistic map of negative motor areas of the upper limb and face: A brain stimulation study. *Brain.* 2019;142(4):952–965.

30. Glasser MF, Coalson TS, Robinson EC, et al. A multi-modal parcellation of human cerebral cortex. *Nature.* 2016;536(7615): 171–178.

31. Glasser MF, Van Essen DC. Mapping human cortical areas in vivo based on myelin content as revealed by T1-and T2-weighted MRI. *J Neurosci.* 2011;31(32):11597–11616.

32. Duffy J. *Differential diagnosis, and management.* Motor speech disorders: substrates, 3rd edn. St. Louis, MO: Elsevier, Mosby; 2013.

33. Budisavljevic S, Dell'Acqua F, Djordjilovic V, Miotto D, Motta R, Castiello U. The role of the frontal aslant tract and premotor connections in visually guided hand movements. *Neuroimage.* 2017;146:419–428.

34. Fujii M, Maesawa S, Motomura K, et al. Intraoperative subcortical mapping of a language-associated deep frontal tract connecting the superior frontal gyrus to Broca's area in the dominant hemisphere of patients with glioma. *J Neurosurg.* 2015;122(6):1390–1396.

35. Kinoshita M, de Champfleur NM, Deverdun J, Moritz-Gasser S, Herbet G, Duffau H. Role of fronto-striatal tract and frontal aslant tract in movement and speech: An axonal mapping study. *Brain Struct Funct.* 2015;220(6):3399–3412.

36. Hickok G, Poeppel D. The cortical organization of speech processing. *Nat Rev Neurosci.* 2007;8(5):393–402.

37. Maldonado IL, Moritz-Gasser S, Duffau H. Does the left superior longitudinal fascicle subserve language semantics? A brain electrostimulation study. *Brain Struct Funct.* 2011;216(3):263–274.

38. Martino J, Hamer PCDW, Berger MS, et al. Analysis of the subcomponents and cortical terminations of the perisylvian superior longitudinal fasciculus: A fiber dissection and DTI tractography study. *Brain Struct Funct.* 2013;218(1):105–121.

39. Moritz-Gasser S, Duffau H. The anatomo-functional connectivity of word repetition: Insights provided by awake brain tumor surgery. *Front Hum Neurosci.* 2013;7:405.

40. Duffau H. Stimulation mapping of white matter tracts to study brain functional connectivity. *Nat Rev Neurol.* 2015;11(5): 255–265.

41. Mandonnet E, Winkler PA, Duffau H. Direct electrical stimulation as an input gate into brain functional networks: Principles, advantages and limitations. *Acta Neurochirurg.* 2010;152(2): 185–193.

42. Price CJ. The anatomy of language: A review of 100 fMRI studies published in 2009. *Ann N Y Acad Sci.* 2010;1191:62–88.

43. Herbet G, Moritz-Gasser S, Duffau H. Electrical stimulation of the dorsolateral prefrontal cortex impairs semantic cognition. *Neurology.* 2018;90(12):e1077–e1084.

44. Amunts K, Lenzen M, Friederici AD, et al. Broca's region: Novel organizational principles and multiple receptor mapping. *PLoS Biol.* 2010;8(9):e1000489.

45. Clos M, Amunts K, Laird AR, Fox PT, Eickhoff SB. Tackling the multifunctional nature of Broca's region meta-analytically: Co-activation-based parcellation of area 44. *NeuroImage.* 2013;83: 174–188.

46. Chang EF, Kurteff G, Wilson SM. Selective interference with syntactic encoding during sentence production by direct electrocortical stimulation of the inferior frontal gyrus. *J Cogn Neurosci.* 2018;30(3):411–420.

47. Friederici AD. The neural basis for human syntax: Broca's area and beyond. *Curr Opin Behav Sci.* 2018;21:88–92.

48. Newhart M, Trupe LA, Gomez Y, et al. Asyntactic comprehension, working memory, and acute ischemia in Broca's area versus angular gyrus. *Cortex.* 2012;48(10):1288–1297.

49. Wilson SM, Galantucci S, Tartaglia MC, et al. Syntactic processing depends on dorsal language tracts. *Neuron.* 2011;72(2): 397–403.

50. Zaccarella E, Friederici AD. Merge in the human brain: A sub-region based functional investigation in the left pars opercularis. *Front Psychol*. 2015;6:1818.

51. Gonzálvez GG, Trimmel K, Haag A, et al. Activations in temporal areas using visual and auditory naming stimuli: A language fMRI study in temporal lobe epilepsy. *Epilepsy Res*. 2016;128:102–112.

52. Trimmel K, van Graan AL, Caciagli L, et al. Left temporal lobe language network connectivity in temporal lobe epilepsy. *Brain*. 2018;141(8):2406–2418.

53. Vigneau M, Beaucousin V, Herve PY, et al. Meta-analyzing left hemisphere language areas: Phonology, semantics, and sentence processing. *Neuroimage*. 2006;30(4):1414–1432.

54. Martino J, Brogna C, Robles SG, Vergani F, Duffau H. Anatomic dissection of the inferior fronto-occipital fasciculus revisited in the lights of brain stimulation data. *Cortex*. 2010;46(5):691–699.

55. Martino J, Vergani F, Robles SG, Duffau H. New insights into the anatomic dissection of the temporal stem with special emphasis on the inferior fronto-occipital fasciculus: Implications in surgical approach to left mesiotemporal and temporoinsular structures. *Oper Neurosurg*. 2010;66(3 Suppl Operative):4–12.

56. Sarubbo S, De Benedictis A, Maldonado IL, Basso G, Duffau H. Frontal terminations for the inferior fronto-occipital fascicle: Anatomical dissection, DTI study and functional considerations on a multi-component bundle. *Brain Struct Funct*. 2013; 218(1):21–37.

57. Duffau H, Gatignol P, Mandonnet E, Peruzzi P, Tzourio-Mazoyer N, Capelle L. New insights into the anatomo-functional connectivity of the semantic system: A study using cortico-subcortical electrostimulations. *Brain*. 2005;128(Pt 4): 797–810.

58. Moritz-Gasser S, Herbet G, Duffau H. Mapping the connectivity underlying multimodal (verbal and non-verbal) semantic processing: A brain electrostimulation study. *Neuropsychol*. 2013; 51(10):1814–1822.

59. Floel A, Buyx A, Breitenstein C, Lohmann H, Knecht S. Hemispheric lateralization of spatial attention in right- and left-hemispheric language dominance. *Behav Brain Res*. 2005; 158(2):269–275.

60. Knecht S, Drager B, Deppe M, et al. Handedness and hemispheric language dominance in healthy humans. *Brain*. 2000;123 Pt 12:2512–2518.

61. Shum J, Fanda L, Dugan P, Doyle WK, Devinsky O, Flinker A. Neural correlates of sign language production revealed by electrocorticography. *Neurology*. 2020;95(21):e2880–e2889.